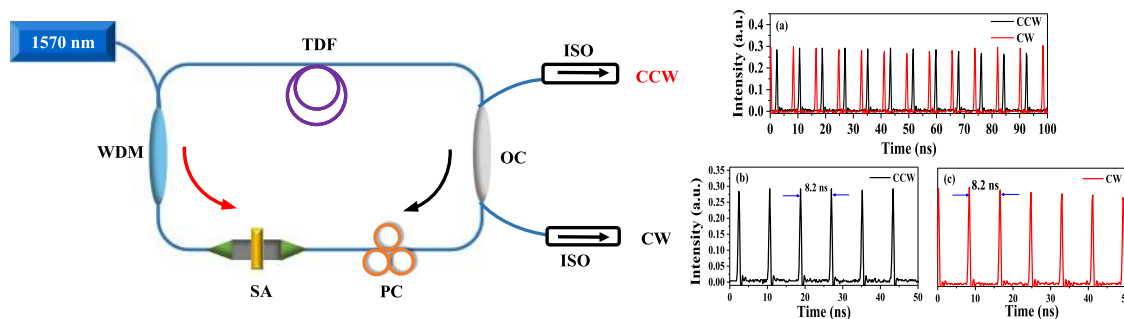


All-Fiber Bidirectional Mode-Locked Ultrafast Fiber Laser at $2 \mu\text{m}$





Volume 11, Number 6, December 2019

Yiming Li
Ke Yin
Xin Zhang
Xin Zheng
Xiangai Cheng
Tian Jiang



DOI: 10.1109/JPHOT.2019.2957167

All-Fiber Bidirectional Mode-Locked Ultrafast Fiber Laser at 2 μm

Yiming Li ¹, Ke Yin ^{2,3}, Xin Zhang ¹, Xin Zheng,²
Xiangai Cheng,¹ and Tian Jiang ¹

¹College of Advanced Interdisciplinary Studies, National University of Defense Technology, Changsha 410073, China

²National Innovation Institute of Defense Technology, Academy of Military Sciences PLA China, Beijing 100071, China

³State Key Laboratory of High Performance Computing, College of Computer, National University of Defense Technology, Changsha 410073, China

DOI:10.1109/JPHOT.2019.2957167

This work is licensed under a Creative Commons Attribution 4.0 License. For more information, see <https://creativecommons.org/licenses/by/4.0/>

Manuscript received October 28, 2019; revised November 18, 2019; accepted November 26, 2019. Date of publication December 9, 2019; date of current version December 18, 2019. This work was supported in part by the National Natural Science Foundation of China under Grants 61805282, 11802339, and 11504420; in part by the Opening Foundation of State Key Laboratory of High Performance Computing under Grant 201601-02; in part by the Open Research Fund of Hunan Provincial Key Laboratory of High Energy Technology under Grant GNJGJS03; in part by the Opening Foundation of State Key Laboratory of Laser Interaction with Matter under Grant SKLLIM1702; and in part by the China Postdoctoral Innovation Science Foundation under Grant BX20180373. Corresponding author: Tian Jiang (e-mail: tjjiang@nudt.edu.cn).

Abstract: In this paper, we demonstrated an all-fiber bidirectional ultrafast thulium-doped fiber laser at 2 μm with a single-wall carbon nanotube presented as saturable absorber. We successfully obtained bidirectional mode-locking operations with pulse repetition frequency adjustable from 35 to 122 MHz by shortening the cavity length. Meanwhile, with the reduction of the intracavity dispersion, the number of Kelly sidebands was significantly decreased and the output energy was more concentrated on the soliton pulse. Besides, by manipulating the pump power and polarization controller, the two results of bidirectional mode-locked pulses with the same repetition frequency and differential repetition frequency were observed. We found that the repetition rate difference between the clockwise and counterclockwise pulse trains was adjustable by changing the pump power or controlling the intracavity polarization. When the pulse repetition frequency was 35 MHz and 122 MHz, the adjustment range of repetition rate difference was 764–922 Hz and 540–2000 Hz, respectively. It is believed that this novel laser source can support free-running dual optical comb spectroscopy to detect important air gases like H_2O or CO_2 in the future.

Index Terms: Ultrafast lasers, fiber optics and oscillators, thulium-doped fiber, infrared and far-infrared lasers.

1. Introduction

Currently, the applications of femtosecond lasers have greatly expanded from time-resolved spectroscopy [1] to materials processing and manufacturing, microscopy [2], biomedical imaging, ranging and dimensional metrology, timing and synchronization, optical communication, and remote sensing. When comparing with other ultrafast lasers, the passively mode-locked ultrafast fiber lasers are simpler to implement, more lightweight, more compact, lower cost, longer-term stable, more robust, and more effective in thermal management. Insights into the frequency-domain picture of optical pulse trains have culminated in the concept of optical frequency combs, which can output

evenly spaced longitudinal modes with an extremely high accuracy. Since the optical frequency comb was first proposed more than a decade ago, it profoundly impacted on various ultra-precise scientific fields, such as metrology and spectroscopy.

Recently, the development of dual-comb mode-locked laser allows rapid acquisition of molecular spectra with high resolution, which also furnishes a powerful method in gas detection. Dual-comb spectroscopy (DCS) usually relies on the generation of two frequency combs, which have slightly different repetition rates between each other. The optical characteristics are thus down-converted in a photodetector into a radio frequency (RF) signal at high sampling speeds without requiring any moving optical parts, since the single fast photodetector is not able to correspond to optical frequency directly. However, DCS is limited by its complex and large system for considering that the pulses are emitted by two independent lasers at the beginning of its generation, which are phase locked to each other tightly. With the rapid development of different laser multiplexing techniques, the free-running dual-comb lasers [3]–[8] have been proved to be effective tools for DCS, which make possible for the direct generation of two high-stability mode-locked laser outputs with different repetition frequencies from a single cavity [3], [9], [10]. Additionally, single cavity dual combs have demonstrated great potentials in gas detection [3], [5], [9], [11], [12]. As the two combs are generated from a single cavity, intrinsic phase coherence and no requirement for complicated servo locking systems enable compact and low-complexity DCS.

In fact, the 2 μm wavelength region covers various gas absorption lines, a few important gas test results are already reported, such as CO_2 , H_2O and CH_4 [3], [13]. In 2018, Kieu *et al* [3] have demonstrated a bidirectional mode-locked thulium-doped fiber laser as a single-cavity dual-comb source, which implemented a 1.47 m-long air path to detect atmospheric H_2O . However, in their work the lasing wavelength was at 1870 nm. It is attractive if the lasing wavelength is shifted to the longer region of 1950–2100 nm [14] as it may finally be converted to the 3–5 μm fingerprint mid-infrared region by using a sub-harmonic optical parametric oscillator [15]. With the development of mid-infrared optical comb, DCS will be increasingly accessible for more important fields such as air pollution monitoring and respiratory gas detection. Thus, researches on single cavity dual-comb mode-locking at 2 μm have meaningful significances.

To date, there are three major approaches to realize dual-comb lasing in a single fiber laser, which are the wavelength multiplexing [16], [17], the polarization multiplexing [18]–[21] and the bidirectional mode-locking [3], [6], [22]. The combination of soliton mode-locking with a saturable absorber (SA) [23] implies a simple and robust cavity construction, which considered to be feasible in operation. Along with deep researches and characterization on novel materials [24], [25], the nonlinear absorption characteristic of materials has been intensively studied [26], [27]. By inserting a saturated absorber, the fiber laser cavity could remain very stable and easily realize self-starting. In this work, a single-wall carbon nanotube (SWNT) film is selected as the SA for a bidirectional mode-locked thulium-doped fiber laser. Benefiting from the robust properties of SWNT film, long-term operations of soliton mode-locked pulses at 1960 nm are demonstrated. In experiments, the repetition rate difference between the clockwise (CW) and counterclockwise (CCW) pulse trains was adjustable by changing the pump power or controlling the intracavity polarization. The experimental setup is presented in detail in Section 2. Experimental results and discussions are shown in Section 3. In the end, the main conclusions of this work are summarized in Section 4.

2. Experimental Setup

The configuration of this bidirectional mode-locked ultrafast fiber laser is illustrated in Fig. 1 schematically. The laser cavity consists of a 20 cm-long piece of thulium fiber (TDF, with a core diameter of 5 μm , a core NA of 0.24, a core absorption of 330 dB/m at 1570 nm) as gain medium, a 1570 nm fiber laser (maximum output power 2 W) as the pump light, a 2×2 optical coupler (OC, splitting ratio of 10:90 at 1960 nm) as the laser pulse output ports, a single-wall CNT film selected as SA, inserted between two fiber connectors and directly fusion spliced into the laser cavity. The preparation method of CNT-SA film is similar to a previous work in 2013 [28]. The

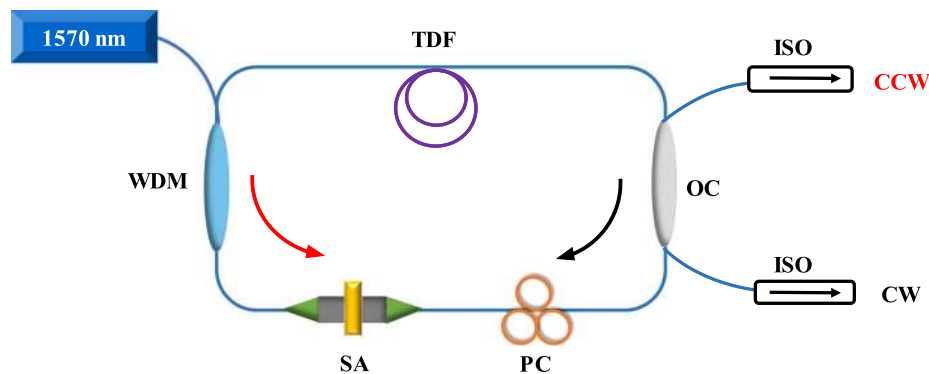


Fig. 1. Schematic diagram of the bidirectional dual-comb mode-locked thulium-doped fiber laser. WDM: 1570/1960 nm wavelength division multiplexer; TDF: thulium-doped fiber; SWNT-SA: single-wall carbon nanotube based saturable absorber; PC: polarization controller; OC: optical coupler; ISO: isolator; CW: clockwise; CCW: counter clockwise.

pump light is coupled to the TDF via a 1570/1960 nm wavelength division multiplexer (WDM). The 10% splitting ports of the OC are used for the extraction of laser pulse in both CW and CCW directions. Two isolators (ISOs) are spliced with these outputs to eliminate any possible optical feedback and enhance the operation stability. Meanwhile, a polarization controller (PC) is used to control the intracavity polarization evolution in order to lock the pulses for long-term operation. The gain TDF has a dispersion of $-67 \text{ ps}^2/\text{km}$ at 1960 nm, while the other fibers are the same passive single-mode fiber with a dispersion of $-80 \text{ ps}^2/\text{km}$ at 1960 nm. Therefore, total dispersion is calculated to be anomalous and the mode-locking scheme belongs to ordinary soliton mode-locking.

In the experiment, the output power is measured with a power meter. The optical spectra of the mode-locked laser pulses are recorded by a grating based optical spectrum analyzer (spectral resolution of 0.05 nm). The output pulse trains are also measured with two $2 \mu\text{m}$ InGaAs detectors monitored on a 1 GHz oscilloscope. Other measuring equipment includes a RF spectrum analyzer. To characterize the combined spectrum and RF spectrum of the CW and CCW laser pulses, a 50:50 OC is used to combine them.

3. Experimental Results and Discussion

In the work, the cavity length was $\sim 5.7 \text{ m}$ at first, and the total dispersion was calculated at -0.45 ps^2 . By increasing the pump power from 0 to 400 mW, amplified spontaneous emission light and self-lasing at both directions with output spectrum peaked at 1960 nm were observed first. By increasing the pump power to 450 mW, self-starting mode-locking operation in the CCW direction was obtained even without adjusting the PC. But the output in the CW direction was continuous. On the one hand, this phenomenon was attributed to the intracavity gain competition between the two directions. On the other hand, because the SA was commonly shared by two directions, it induced crosstalk into the cavity that leading to obvious pulse competition, contributing such apparently different performance of two directions. When increasing the pump power to 550 mW, along with carefully adjusting the PC, the aforementioned competition was weakened. At this time, ultrafast laser pulses were monitored from both directions shown in Fig. 2. The separation between adjacent pulses was around 28.6 ns, corresponding to the cavity length of 5.7 m. When the resolution was 10 Hz, the combined RF spectrum was measured as shown in Fig. 2(d). The SNR (signal noise ratio) of the signals was $\sim 50 \text{ dB}$ at the repetition frequencies of 35.148 and 35.149 MHz for the CW and CCW directions, respectively. The output power of CW and CCW arm was 650 and 611 μW .

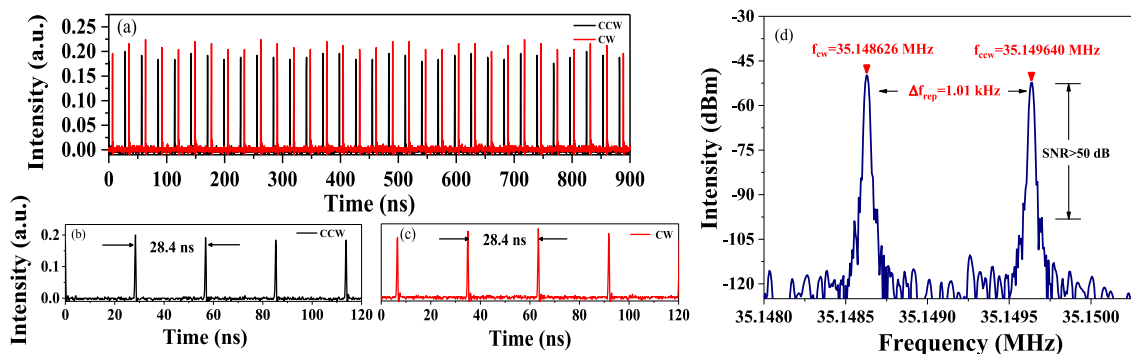


Fig. 2. Output characteristics of bidirectional mode-locking operation with repetition frequency of 35 MHz. (a) Output pulses of CCW and CW directions in time domain. (b) Zoom of pulse trains in CCW direction with spacing of 28.4 ns. (c) Zoom of pulse trains in CW direction with spacing of 28.4 ns. (d) RF of fundamental bidirectional mode-locking pulses with ~ 50 dB SNR measured with 10 Hz RBW.

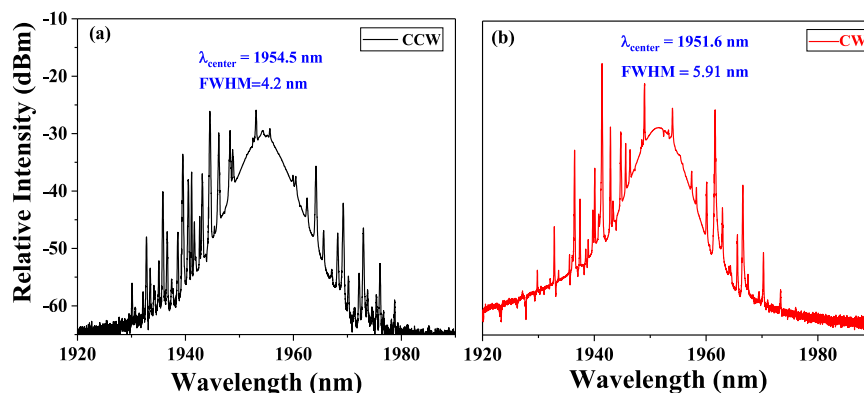


Fig. 3. Output characteristics of bidirectional mode-locking operation with repetition frequency of 35 MHz. (a) Spectrum of CCW direction. (b) Spectrum of CW direction.

Fig. 3 shows the measured spectral characteristics of the bidirectional mode-locking operation with the repetition frequency of 35 MHz. Obviously, the output smooth spectra suggest the ultrafast soliton mode-locking operations, accompanied by numerous Kelly sidebands. However, due to the large anomalous dispersion, a fierce competition between the soliton pulse and the quasi-continuous Kelly sidebands occur. Therefore, we find that the bidirectional mode-locking operation could not sustain for long time. As a result, the output in the CW direction often decayed into continuous wave lasing.

To solve the aforementioned problem, we adopted the dispersion management to decrease the cavity dispersion and improve the output spectral purities. Typically, there are two commonly adopted methods to compensate the dispersion in an ultrafast fiber laser cavity, either by adding a piece of dispersion compensation fiber (DCF) or shortening the effective cavity length. In this work, due to the lack of DCF at 2 μm , thus we ameliorated the dispersion by cutting these passive fibers. With the shortening of the cavity length, the intracavity total dispersion usually decreased, allowing for the narrower soliton pulse duration and the much broader Kelly sidebands spacing.

Followed by the previous step, we reduced the cavity length to 2.9 m. At this time, the repetition frequency was scaled up to ~ 68 MHz, and similar bi-directional mode-locking operations were observed. When the cavity length was further shortened to ~ 1.7 m and the pump power was set to 725 mW with an appropriate PC state, the bi-directional mode-locking operations could still be observed. The corresponding pulse repetition frequency increased up to ~ 122 MHz. The pulse

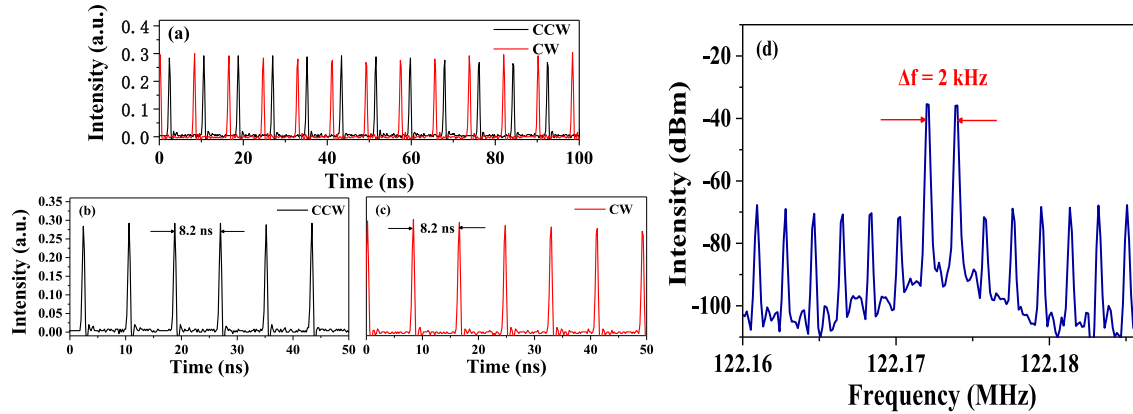


Fig. 4. Output characteristics of bidirectional mode-locking operation with repetition frequency of 122 MHz. (a) Output pulses of CCW and CW directions in time domain. (b) Zoom of pulse trains in CCW direction with spacing of 8.2 ns. (c) Zoom of pulse trains in CW direction with spacing of 8.2 ns. (d) RF of fundamental bidirectional mode-locking pulses with ~ 60 dB SNR measured with 10 Hz RBW.

trains from both directions were measured with the results shown in Fig. 4. By analyzing the RF spectrum (see Fig. 4(d)), bidirectional mode-locking pulses with ~ 60 dB SNR were measured with 10 Hz RBW, indicating a more stable mode-locking operation compared with that at long cavity length. The fundamental repetition rates of CW and CCW directions were 122.172 and 122.174 MHz, respectively. The measured repetition rate difference (Δf_{rep}) from both directions was ~ 2 kHz. As illustrated in Fig. 4(b) and (c), the separation between adjacent pulses was around 8.2 ns, corresponding to the cavity length of 1.7 m. The output power from CW and CCW directions was 1.547 and 1.001 mW respectively.

When the cavity length was shortened to 1.7 m, the calculated intracavity dispersion decreased to -0.13 ps², which was reduced comparing with that at 5.7 m. The shortening of passive fiber length contributed to the decrease of intracavity anomalous dispersion. Thus, fewer Kelly sidebands were displayed and the spectra became smooth in both directions as shown in Fig. 5. The minimum difference of the central wavelengths between CW and CCW pulses was ~ 2.7 nm. Their central wavelengths were 1958.2 and 1955.5 nm, respectively. The 3-dB bandwidths of the optical spectra were 7.53 and 4.87 nm. Our experimental observations showed that the central wavelengths of the counterpropagating pulses of bidirectional operation were different in most cases. Nevertheless, via continuously increasing the pump power to 855 mW, the central wavelengths of the counterpropagating pulses could be identical. In this case, the bidirectional mode-locked laser operated in the single-wavelength direction-multiplexed mode-locking regime (see Fig. 5(d)), so that the spectra of the two frequency combs could overlap without extra-cavity nonlinear spectral broadening. The theoretical repetition rate difference (Δf_{rep}) from both directions was calculated as 2.69 kHz according to the formula 3 in Ref. [6], the relationship between Δf_{rep} and two directions wavelength difference ($\Delta\lambda$) can be expressed as

$$\Delta f_{rep} = \frac{LD\Delta\lambda}{t^2} \quad (1)$$

Here D refers to dispersion of the SMF and TDF, given as 40 and 35 ps/(nm·km) in our experiment. The observed round-trip time t was ~ 8.2 ns. The total cavity length L and $\Delta\lambda$ are 1.7 m and 2.7 nm, respectively.

The time-bandwidth product of a pulse refers to the product of its time domain pulse width (Δt) and spectral width ($\Delta\nu$). The minimum time-bandwidth product of a hyperbolic secant pulse is

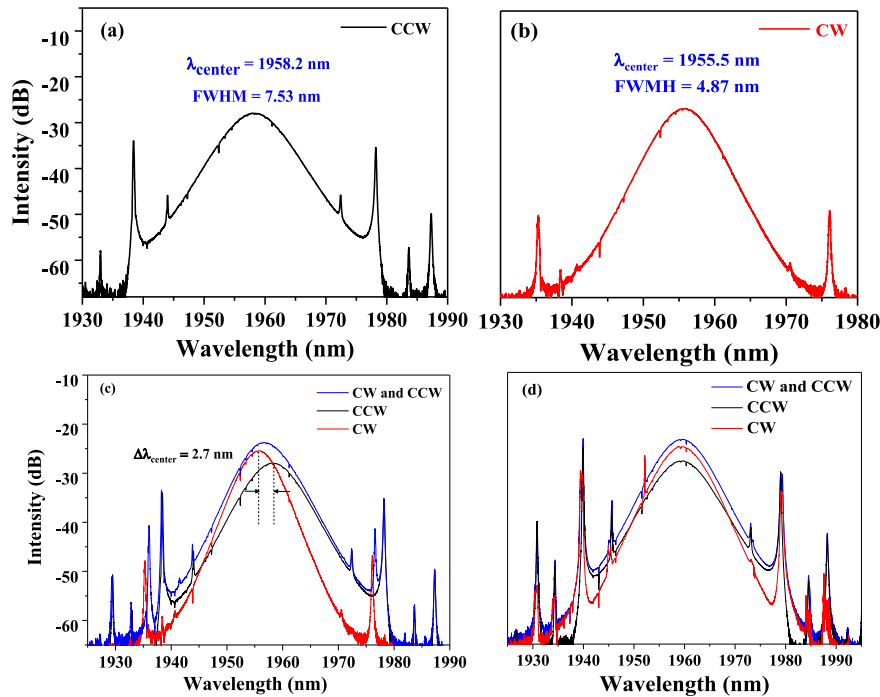


Fig. 5. Output spectra characteristics of bidirectional mode-locking operation with repetition frequency of 122 MHz. (a) Spectrum of CCW at 122 MHz. (b) Spectrum of CW at 122 MHz. (c) Spectra of CW and CCW at 122 MHz with 2.7-nm center wavelength offset. (d) Spectrum of CW and CCW at 122 MHz with center wavelength coincides.

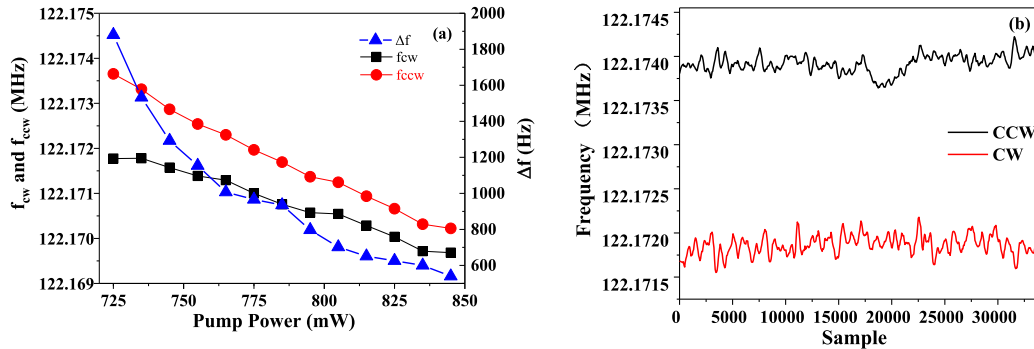


Fig. 6. (a) Variation of repetition frequency with pump power from 725 to 850 mW. (b) Frequency stability over 9 h at 122 MHz.

approximately 0.315 shown in formula (2).

$$\Delta\nu \times \Delta t = 0.315 \quad (2)$$

Thus, for a given spectral width, the time domain pulse width has a minimum limit. This limitation is determined by the nature of the Fourier transform. In ultrafast laser physics, pulse width and spectral width are usually referred to full width at half maximum (FWHM). In the experiment, the measured FWHM ($\Delta\lambda$) of CW and CCW directions is 4.87 and 7.53 nm, respectively. As is known,

$$\Delta\nu = \frac{c \times \Delta\lambda}{\lambda^2} \quad (3)$$

Therefore, according to formula (2) and (3), the corresponding pulse width in time domain (Δt) is 824 and 530 fs, respectively.

Fig. 6(a) depicted the variation of repetition frequency with pump power from 725 to 850 mW. With larger pump power, both the repetition frequency and Δf_{rep} declined. Limited by the range of pump regulation, the minimum Δf_{rep} that processed in the experiment was 540 Hz along with tuning the PC. In addition, the stability of our bi-directional mode-locked laser was also examined, as illustrated in Fig. 6(b). The sampling interval was set to one sampling point per second. Experimental observations confirmed that the proposed TDF laser could operate at a stable bi-directional mode-locking state for more than 9 h.

4. Conclusions

In summary, we have proposed and experimentally implemented a bidirectional mode-locked fiber laser based on SWNT. By properly changing the cavity length and altering pump power, we successfully achieved an adjustable repetition frequency range from 35 MHz to 122 MHz. Besides, the optical spectra and RF spectra of different repetition rates were also performed. It is worth noting that the CW and CCW pulses have different repetition rates with the smallest separation of ~ 540 Hz at 122 MHz. The central wavelengths of the counterpropagating pulses could be the same via appropriately tuning the PC and pump power. Furthermore, the bidirectional mode-locking operation was examined with a 9-hour stability. We believe that this light source might be supported with 2 μm and mid-infrared dual optical combs in the future.

References

- [1] I. Kudelin, S. Sugavanam, and M. Chernysheva, "Real-time observation of soliton build-up dynamics in bidirectional mode-locked fibre lasers," (in English), in *Proc. Conf. Lasers Electro-Opt.*, 2019, Paper STu3L.7.
- [2] H. Hao *et al.*, "Visualized charge transfer processes in monolayer composition-graded $\text{WS}_{2-x}\text{Se}_{2(1-x)}$ lateral heterojunctions via ultrafast microscopy mapping," *Opt. Exp.*, vol. 26, no. 12, pp. 15867–15886, Jun. 2018.
- [3] J. Olson, Y. H. Ou, A. Azarm, and K. Kieu, "Bi-directional mode-locked thulium fiber laser as a single-cavity dual-comb source," *IEEE Photon. Technol. Lett.*, vol. 30, no. 20, pp. 1772–1775, Oct. 2018.
- [4] K. Kieu and M. Mansuripur, "All-fiber bidirectional passively mode-locked ring laser," *Opt. Lett.*, vol. 33, no. 1, pp. 64–66, Jan. 2008.
- [5] S. Mehravar, R. A. Norwood, N. Peyghambarian, and K. Kieu, "Real-time dual-comb spectroscopy with a free-running bidirectionally mode-locked fiber laser," *Appl. Phys. Lett.*, vol. 108, no. 23, 2016, Art. no. 231104.
- [6] C. Zeng, X. Liu, and L. Yun, "Bidirectional fiber soliton laser mode-locked by single-wall carbon nanotubes," *Opt. Exp.*, vol. 21, no. 16, pp. 18937–18942, Aug. 2013.
- [7] K. Zhao, H. Jia, P. Wang, J. Guo, X. Xiao, and C. Yang, "Free-running dual-comb fiber laser mode-locked by nonlinear multimode interference," *Opt. Lett.*, vol. 44, no. 17, pp. 4323–4326, Sep. 2019.
- [8] M. I. Kayes, N. Abdukerim, A. Rekik, and M. Rochette, "Free-running mode-locked laser based dual-comb spectroscopy," *Opt. Lett.*, vol. 43, no. 23, pp. 5809–5812, Dec. 2018.
- [9] R. Liao, Y. Song, W. Liu, H. Shi, L. Chai, and M. Hu, "Dual-comb spectroscopy with a single free-running thulium-doped fiber laser," *Opt. Exp.*, vol. 26, no. 8, pp. 11046–11054, Apr. 2018.
- [10] X. Zhao, Z. Zheng, Y. Liu, G. Hu, and J. Liu, "Dual-wavelength, bidirectional single-wall carbon nanotube mode-locked fiber laser," *IEEE Photon. Technol. Lett.*, vol. 26, no. 17, pp. 1722–1725, Sep. 2014.
- [11] O. Kara, Z. Zhang, T. Gardiner, and D. T. Reid, "Dual-comb mid-infrared spectroscopy with free-running oscillators and complete optical calibration from a radio-frequency reference," in *Proc. Conf. Lasers Electro-Opt.*, 2017, pp. 1–2.
- [12] J. Nurnberg, C. G. E. Alfieri, Z. Chen, D. Waldburger, N. Picque, and U. Keller, "An unstabilized femtosecond semiconductor laser for dual-comb spectroscopy of acetylene," *Opt. Exp.*, vol. 27, no. 3, pp. 3190–3199, Feb. 2019.
- [13] J. Chen *et al.*, "Dual-comb spectroscopy of methane based on a free-running Erbium-doped fiber laser," *Opt. Exp.*, vol. 27, no. 8, pp. 11406–11412, Apr. 2019.
- [14] R. Li, J. Li, L. Shterengas, and S. D. Jackson, "Highly efficient holmium fibre laser diode pumped at 1.94 μm ," *Electron. Lett.*, vol. 47, no. 19, pp. 1089–1090, 2011.
- [15] A. V. Muraviev, V. O. Smolski, Z. E. Loparo, and K. L. Vodopyanov, "Massively parallel sensing of trace molecules and their isotopologues with broadband subharmonic mid-infrared frequency combs," *Nature Photon.*, vol. 12, no. 4, pp. 209–214, 2018.
- [16] X. Zhao *et al.*, "Picometer-resolution dual-comb spectroscopy with a free-running fiber laser," *Opt. Exp.*, vol. 24, no. 19, pp. 21833–21845, Sep. 2016.
- [17] Z.-C. Luo *et al.*, "Tunable multiwavelength passively mode-locked fiber ring laser using intracavity birefringence-induced comb filter," *IEEE Photon. J.*, vol. 2, no. 4, pp. 571–577, Aug. 2010.
- [18] X. Zhao, Z. Gong, Y. Liu, Y. Yang, G. Hu, and Z. Zheng, "Coherent dual-comb mode-locked fiber laser based on a birefringent ring cavity," in *Proc. Frontiers Opt.*, 2015, Paper FW3C.3.

- [19] A. E. Akosman and M. Y. Sander, "Dual comb generation from a mode-locked fiber laser with orthogonally polarized interlaced pulses," *Opt. Exp.*, vol. 25, no. 16, pp. 18592–18602, Aug. 2017.
- [20] S. M. Link *et al.*, "Dual-comb modelocked laser," *Opt. Exp.*, vol. 23, no. 5, pp. 5521–31, Mar. 2015.
- [21] Y. Nakajima, Y. Hata, and K. Minoshima, "All-polarization-maintaining, polarization-multiplexed, dual-comb fiber laser with a nonlinear amplifying loop mirror," *Opt. Exp.*, vol. 27, no. 10, pp. 14648–14656, 2019.
- [22] S. Saito, M. Yamanaka, Y. Sakakibara, E. Omoda, H. Kataura, and N. Nishizawa, "All-polarization-maintaining Er-doped dual comb fiber laser using single-wall carbon nanotubes," *Opt. Exp.*, vol. 27, no. 13, pp. 17868–17875, 2019.
- [23] J. Sotor, G. Sobon, I. Pasternak, A. Krajewska, W. Strupinski, and K. M. Abramski, "Simultaneous mode-locking at 1565 nm and 1944 nm in fiber laser based on common graphene saturable absorber," *Opt. Exp.*, vol. 21, no. 16, pp. 18994–9002, Aug. 2013.
- [24] C. Zhang *et al.*, "Anisotropic nonlinear optical properties of a SnSe flake and a novel perspective for the application of all-optical switching," *Adv. Opt. Mater.*, vol. 7, no. 18, 2019, Art. no. 1900631.
- [25] J. Zhang *et al.*, "Ultrafast saturable absorption of MoS₂ nanosheets under different pulse-width excitation conditions," *Opt. Lett.*, vol. 43, no. 2, pp. 243–246, Jan. 15 2018.
- [26] R. Miao *et al.*, "Ultrafast nonlinear absorption enhancement of monolayer MoS₂ with plasmonic Au nanoantennas," *Opt. Lett.*, vol. 44, no. 13, pp. 3198–3201, Jul. 2019.
- [27] J. Zhang *et al.*, "Saturated absorption of different layered Bi₂Se₃ films in the resonance zone," *Photon. Res.*, vol. 6, no. 10, pp. C8–C14, 2018.
- [28] M. Zhang *et al.*, "Mid-infrared Raman-soliton continuum pumped by a nanotube-mode-locked sub-picosecond Tm-doped MOPFA," *Opt. Exp.*, vol. 21, no. 20, pp. 23261–23271, Oct. 2013.